Tribochemistry of overbased calcium detergents studied by ToF-SIMS and other surface analyses

L. Cizaire[a,*], J.M. Martin[a], E. Gresser[b], N. Truong Dinh[c] and C. Heau[d]

[a]Ecole Centrale de Lyon, LTDS, 36 Avenue Guy de Collongue, 69134 Ecully, France
[b]Total, Centre de Recherche de Solaize (CReS), 69360 Solaize, France
[c]Condat Lubrifiants, avenue Frédéric Mistral, 38670 Chasse Sur Rhone, France
[d] H.E.F, rue benoît Fourneyron, 42166 Andrezieux-Boutheon, France

Received 21 September 2003; accepted 16 May 2004

Overbased detergents are well known in the tribology field as anti-wear additives. In boundary lubrication, they generate a quite thick tribofilm on rubbing surfaces. They were studied by coupling XPS and AES depth profiles with XANES and ToF-SIMS analyses. Under friction, we show by ToF-SIMS analysis that detergent molecules are split into smaller structural units. Moreover, ionic bonds do not resist high pressure and shearing, and sulfur disappears from the contact zone. The overbased calcium carbonate core finally collapses and crystallizes to give a good anti-wear film between rubbing surfaces.

KEY WORDS: overbased detergents, ToF-SIMS, XPS, AES, XANES, tribology, anti-wear

1. Introduction

The lubrication of modern internal combustion engines requires the addition of specific additives to the base oil in order to improve the overall engine performance: such as minimization of corrosion, deposits and varnish formation in the engine hot areas. This detergency role is assumed by overbased detergents such as overbased calcium alkylbenzene sulfonate (OCABS). In order to obtain this type of colloidal particle, carbonation of calcium hydroxide in solution is carried out in the presence of alkylbenzene sulfonate (ABS) surfactant. The reaction leads to well-defined nanoparticles. This complex micellar structure has been examined by coupling XPS, ToF-SIMS and EF-TEM (Energy Filtered Transmission Electron Microscopy) [1]. The result is an accurate picture of the localisation of each expected molecular species in the nanoparticle and the quantification of each species. We have shown that OCABS is made of an amorphous core of calcium carbonate surrounded by a shell of didodecylbenzene sulfonate molecules. The amorphous character of the mineral core is due to the presence of calcium hydroxide as an impurity, more concentrated from the centre to the exterior, with a pure corona of calcium hydroxide between the core and the surfactant molecules. Main analytical data are summarized in figure 1. Overbased calcium alkylbenzene sulfonates (OCABS) possess anti-wear properties in the boundary lubricating regime [2–6]. Their anti-wear properties depend on their colloidal structure [7] and on their overbased character [8]. Studies of tribological properties, as well as chemical and structural analyses of OCABS tribofilm have allowed the proposal of a reaction mechanism for the anti-wear film formation. These micelles are first adsorbed on rubbing surfaces and then crystallize [3]. OCABS tribofilms have better mechanical properties than dialyzed micelles because of the crystallization of the mineral cores [9]. Analyses of wear particles by EFTEM show the presence of crystallized calcite grains separated by a homogenous pseudo-graphitic layer [4]. Shearing is controlled by carbon grains to prevent cracking, plastic deformation and abrasion [10]. Amounts of carbon and sulfur, as determined by EELS, decrease in wear particles [11]. The iron concentration is very low, highlighting the good anti-wear properties of OCABS. Results (crystallization of calcium carbonate core and surfactant chains changes) are confirmed by PM-IRRAS analyses (Polarization Modulated Infrared Reflection Absorption Spectroscopy) [12,13]. The carbon fine structure of wear particles, studied by EELS, is significantly different from dialyzed micelles [4]. However, no paper is devoted to the study of surfactant chains changes. The aim of this paper is to focus on the role of surfactant chains as friction reducers and on their final state.

*To whom correspondence should be addressed.
E-mail: linda.cizaire@rolex.com

2. Experimental

2.1. Materials

OCABS of total base number (TBN) 300 were centrifuged and dialyzed to eliminate impurities such as

1023-8883/04/1100–0715/0

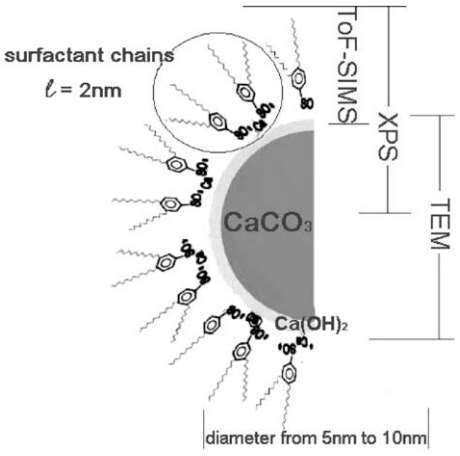

Figure 1. Scheme summarizing analytical data obtained on dialyzed OCABS in previous work [1].

solid particles or light organic molecules. For tribological tests, OCABS were then added to Poly-Alfa Olefin (PAO) base oil at a concentration of 3 wt%. All lubricated tests were carried out with this mixture, whereas for experiments made in UHV conditions, OCABS were tested as a deposited film that was obtained by solvent evaporation from a concentrated solution of OCABS in heptane. Impurities or adsorbed molecules do not pollute rubbing surfaces in UHV conditions, which allows us to analyze, in particular by ToF-SIMS, surfaces in a state characteristic of friction behavior.

2.2. Tribological tests

Friction tests were carried out with a Cameron-Plint tribometer in a cylinder-on-flat configuration. Rubbing surfaces were made of AISI 52100, polished with a 1 μm diamond solution. The experiment runs for 1 h with a stroke length of 7 mm. The mean contact pressure of 850 MPa is applied by a constant normal load of 350 N through the cylinder of 6 mm in diameter. The sliding speed of 200 mm/s is sufficiently low to generate a boundary lubrication regime in the contact area. Lubricant is not heated before friction. The test temperature is about 25 °C and rises to 40 °C at the end of the experiment due to frictional heat.

The second tribometer used in this study has a pin-on-flat contact configuration in UHV environment ($P \cong 10^{-9}$ hPa). Both rubbing surfaces are made of AISI 52100 steel. Maximal contact pressure is about 322 MPa ($F_N = 1$ N) and sliding speed is 0.2 mm/s. Such experimental conditions are quite similar to ones obtained in the boundary lubrication regime. In this test, AISI 52100 pins ($R_c = 8$ mm) were etched before the experiment in order to eliminate layers of native oxide and adventitious carbon. Indeed, we find that, in an ambient environment and lubricated contact, the flat oxide native layer disappears. We would like to determine the role of oxide presence in selective transfer of micelles or in adsorption phenomenon.

2.3. Surface analyses

After friction tests made in an UHV environment, the wear scars on both the pin and the flat are studied by *in-situ* analyses (AES or XPS). AES or XPS depth profiles were performed with Argon ions using an ion gun (VGEX05) operating at 5 keV. Ions irradiate the sample and etch its surface. Auger analyses were carried out using a retard ratio of 4 and a constant primary electron beam current of 5 keV (VG FEG1000). Auger spectra were quantified by determining the peak area in the direct spectrum mode. The XPS measurements were carried out using an AlK_α X-ray source (1486.6 eV). The analyser was operated with a pass energy of 40 eV for oxidation state determination and elemental quantification.

XANES was performed at the Canadian Synchrotron radiation Facility (CSRF), which is located at the Aladdin 1 GeV storage ring, University of Wisconsin, Madison, USA. The Grasshoper beam line was used in this investigation. Regions studied are C–K and Ca–L edges. The X-ray beam is monochromatised by a 1800 g mm^{-1} grating and covers the photon region of 70–900 eV. The energy resolution of this beam line is < 0.3 at 300 eV. Spectra are recorded in fluorescence yield (FY) mode so that the maximum analysis depth is about 5 μm [14].

In ToF-SIMS analysis, the surface of the sample is bombarded by an ion beam provided by a pulsed gallium source working at 25 keV. The atomic and molecular secondary ions are analyzed by mass spectrometry (parallel acquisition with a Time-of-Flight analyzer). Ions coming from the topmost atomic layers can be identified with a time of flight spectrometer giving a mass resolution of 7500 for $m/z = 28$ (silicon wafer).

2.4. Lubricated contact

2.4.1. Wear results

Figure 2 shows the friction coefficient as a function of time for two different lubricants, pure PAO base oil and a mixture of OCABS at 3 wt% in PAO. As can be seen, OCABS have no significant effect on friction compared to PAO base oil. The anti-wear effect of OCABS is highlighted when observing wear tracks by optical microscopy (see images in figure 3). For pure PAO base oil (figure 3(a)), the wear track has a lot of scratches whereas in the case of oil containing OCABS (figure 3(b)), the wear track is quite smooth with a homogenous and thick tribofilm. However, the tribofilm is almost totally removed by water in an ultrasonic bath as shown in figure 4, and this can be

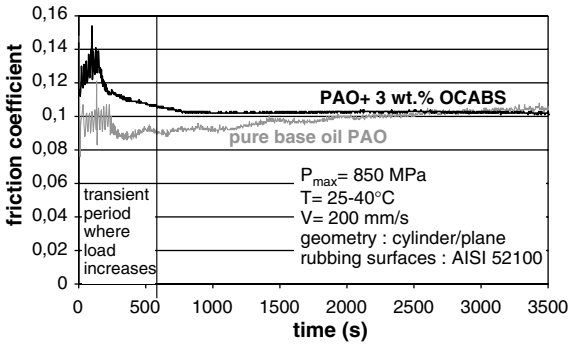

Figure 2. Friction coefficient as a function of time for tribological tests made on Cameron-Plint tribometer.

compared to a simple rinsing with heptane in figure 3(b). No wear scar on the steel substrate is visible below the tribofilm, even on the image obtained in optical microscopy in the dark field mode. The anti-wear effect of micelles becomes indisputable when observing optical images of cylinder wear tracks (see figure 5). Notice that the scales are different by a factor of 4. As a consequence of wear, an important, flat wear scar is observed on the cylinder part after the tribological test with pure PAO. On the other hand, no apparent wear is visible at the end of the experiment when OCABS are added to PAO, since a scratch due to polishing is still present in the contact zone (see the arrow).

2.4.2. Structural and chemical analyses

To determine the thickness of the tribofilm, an AES depth profile of the flat surface was performed. To evaluate the etching speed, the same depth profile was recorded inside and outside the wear scar,

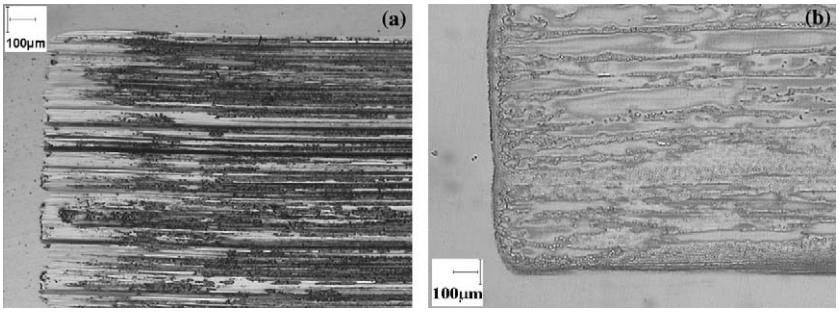

Figure 3. Flat wear tracks observed by optical microscopy (a) with pure base oil, (b) with PAO + 3 wt.% OCABS.

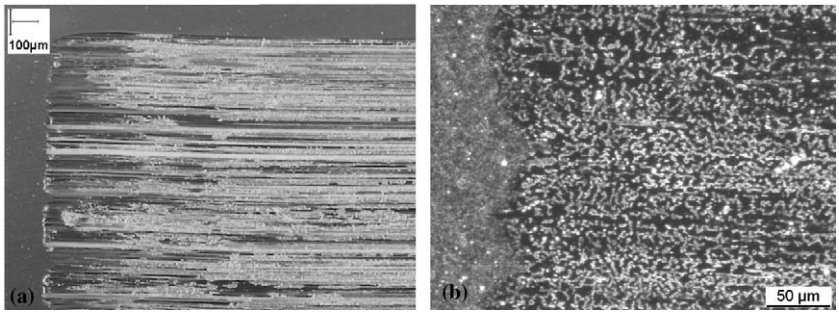

Figure 4. Dark field optical images of flat wear track (a) with pure base oil, a lot of scratches are observed, (b) with micelles, the tribofilm has almost totally disappeared and no wear signs are detected.

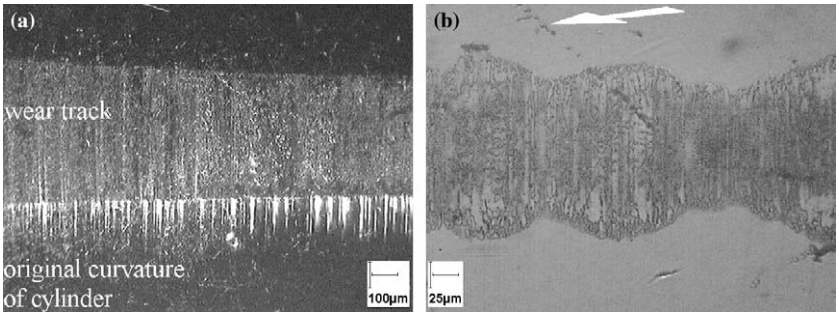

Figure 5. Optical images of cylinders after a test made on a Cameron-Plint tribometer ($P_{max} = 850$ MPa, $T =$ ambient et $V = 200$ mm/s) (a) in the case of pure PAO oil and (b) for PAO + 3 wt.% OCABS. Arrow highlights scratch due to polishing.

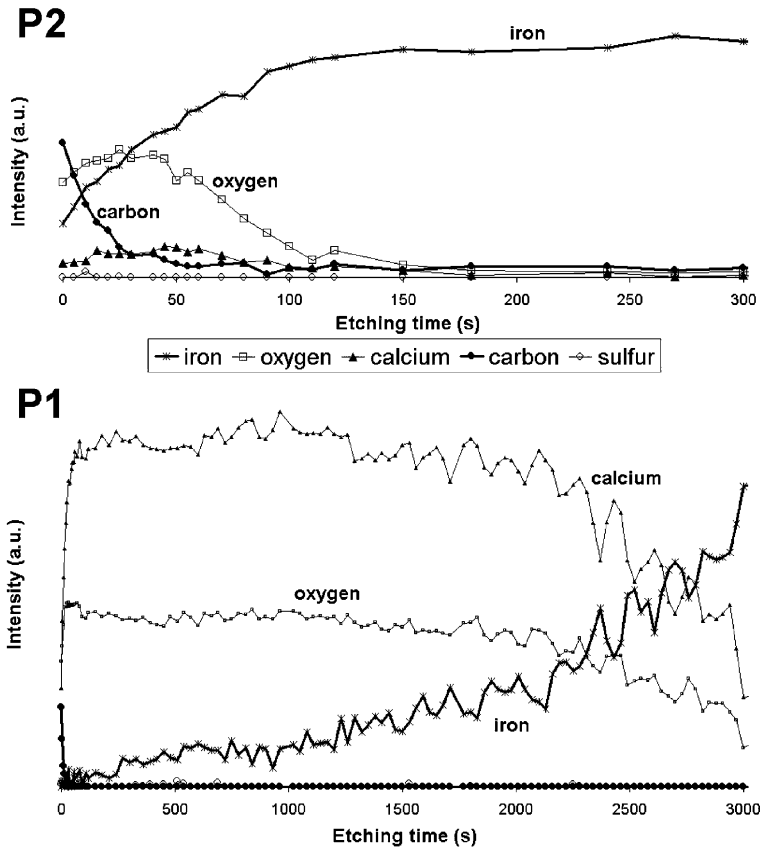

Figure 6. AES profile vs. of the depth time for all elements detected in the tribofilm (P1 point) and outside of the tribofilm (P2 point). The intensity on abscissa was determined with peak areas.

simultaneously. Figure 6 presents the AES profile of the tribofilm (P1 point) and the profile of the native oxide layer of the flat (P2 point). On the P2 point, the main elements detected are oxygen and iron as early as the beginning of the AES profile. The film thickness is found to be 30 times higher than the native oxide layer which is evaluated as 3 nm [15]. Thus, the tribofilm is about 100 nm thick.

The entire tribofilm is composed of calcium carbonate since calcium, carbon and oxygen elements decrease simultaneously along the tribofilm depth (see figure 7). However, the stoichiometry in the XPS profile does not correspond to the theoretical stoichiometry of calcium carbonate. This analysis raises a question: what is the origin of the calcium excess? Previous XPS analyses made on dialyzed OCABS have shown that calcium carbonate is chemically inert to X-rays [1]. This means that calcium carbonate could be detected and quantified. When AES analyses were done, carbon disappears from the system response, showing a high instability of calcium carbonate to electrons. Between these two extreme states, we show here that calcium carbonate is partially reduced by ions into carbon dioxide and calcium oxide. The similar decrease of oxygen in the oxide form with oxygen in the carbonate form agrees with this hypothesis. The excess quantity of calcium corresponds to the quantity of oxygen oxide (see figure 8). It confirms the reduction of a piece of $CaCO_3$ into CaO with evaporation of CO_2.

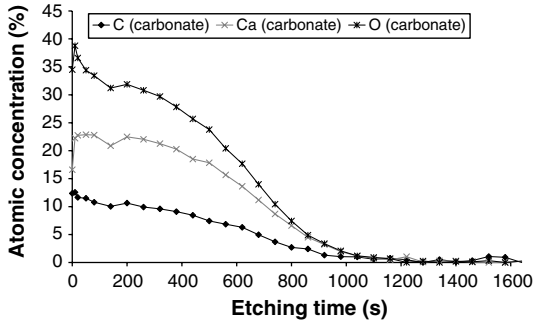

Figure 7. XPS profile based only on calcium carbonate elements (C1s at 290.0 eV, Ca_2p_3 at 347.1 eV and O1s at 532.3 eV).

ToF-SIMS analyses were carried out on lubricated tribofilms and outside wear tracks after rinsing of the surfaces with heptane. We could see that both spectra are similar and correspond to one obtained on dialyzed OCABS (not shown here). It is supposed that adsorbed micelles are still present on mineral and metallic samples (see figure 9). This ''contamination layer'' hides the possible changes to surfactant chains.

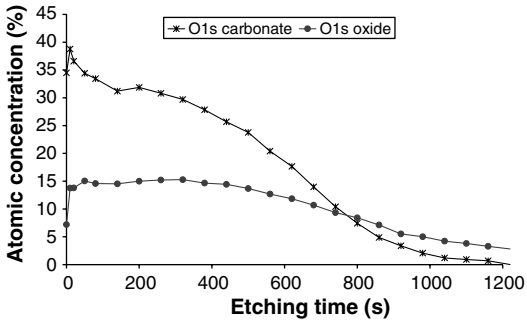

Figure 8. XPS profile of oxide and carbonate oxygen element (O1s at 532.3 eV (carbonate) and 528.2 eV (oxide)).

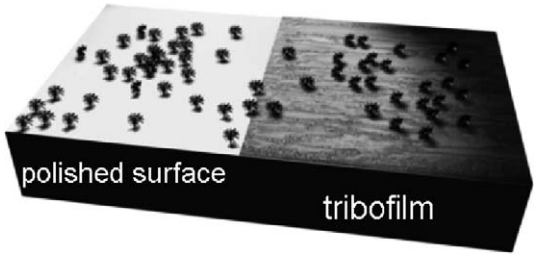

Figure 9. Scheme of incomplete, adsorbed monolayer of micelles on polished ASI 52100 steel and tribofilm.

XANES analyses were done on the Cameron-Plint tribofilm in FY mode, giving an analyzed thickness of 5 μm, in order to get rid of the adsorbed micelles on the specimen. The disappearance of continuum background and the decreasing of a C—H shoulder in figure 10 are some evidence for the surfactant chains expulsion from the tribofilm. The lack of the sulfur element in the XPS depth profile seems to indicate that calcium sulfonate chains have also been expelled from the tribofilm during friction.

The appearance of a 1s/σ*(C—O) transition and the increasing intensity of the 1s/π*(C—O) transition show a chemical transformation of the tribofilm from dialyzed micelles to pure calcite. Peaks 1 (349.2 eV) and 2 (352.5 eV), shown in figure 11, are assigned to the Ca–L edge spin–orbit doublets. Pre-peaks in the

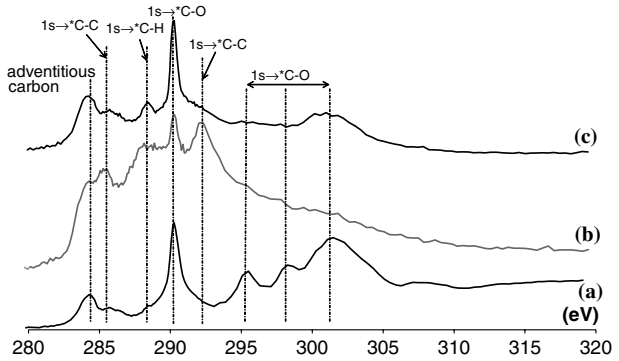

Figure 10. XANES spectra of carbon K-edge on (a) pure calcite, (b) dialyzed micelles and (c) Cameron-Plint tribofilm.

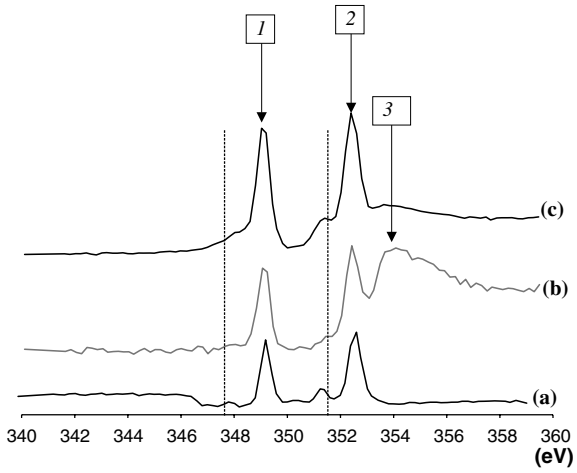

Figure 11. XANES spectra of calcium $L_{2,3}$-edge on (a) pure calcite, (b) dialyzed micelles and (c) Cameron-Plint tribofilm. Note that peak 3 originates from one of the second-order harmonics of the iron L-edge at 712 eV because of the presence of the steel substrate.

tribofilm have grown compared to dialyzed micelles. As they are characteristics of crystallized calcium carbonate, this result indicates that micelles crystallize in the tribofilm in a form more similar to pure calcite than has be shown in previous work [9,13].

2.5. Tribological test with OCABS as deposited film (UHV environment)

It is well known that micelles are capable of instantaneous adsorption on to metallic surfaces that they have been in contact with. We show that they were adsorbed on mineral surfaces, hiding in ToF-SIMS analyses the possible changes of surfactant chains. An ideal experiment with no gas and contact pollution is thus required. OCABS adsorbed film, obtained by solvent evaporation, was, thus, tribologically tested in an UHV environment.

2.5.1. Wear results

The steady-state friction coefficient is very similar to the one obtained for a lubricated contact (see figure 12). We can also suppose that the chemical and

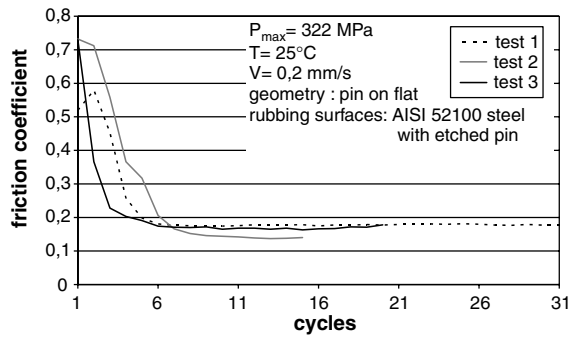

Figure 12. Friction coefficient evolution as a function of cycle number for experiments made in UHV conditions on micelles coating.

structural states of tribofilm are quite identical to those obtained after tests with solutions of both oil and micelles.

2.5.2. Structural and chemical analyses

ToF-SIMS analysis, with its sensitivity to the first top monolayer, permits a focus on evolutions of surfactant chains. ToF-SIMS spectra obtained on flat wear tracks highlight that fewer long surfactant chains are still present after the friction experiment (figure 13). The peak due to hydrocarbon chains containing eight carbons has a higher intensity than for dialyzed micelles and is duplicated. This new peak ($C_8H_9SO_3$) corresponds to a stable chemical unit of initial surfactant chain and proves the splitting of surfactant chains during friction.

3. Discussion

Added to base oils like PAO, OCABS prevent wear of rubbing surfaces by growing an anti-wear tribofilm in the contact zone. A steady-state behavior is achieved as long as new additives enter the contact and replenish the tribofilm. OCABS could protect surfaces better than ZDDP in terms of wear rate, which corresponds to losses of volume, [4] as OCABS do not need to be thermally activated. They have moreover many advantages compared, for example, to ZDDP. They protect surfaces even at low temperature (ambient temperature) and do not have a transient period during which the wear rate is very high.

The formation of tribofilm is made up of three stages depending on contact severity as depicted in figure 14:

(1) For lower pressure and shearing, long hydrocarbon surfactant chains are split into smaller units.
(2) At higher contact pressure or for longer sliding distance, the ionic bonds between sulfur and calcium are broken. The Sulfur element is expelled out of the tribofilm leaving, however, some carbon species.

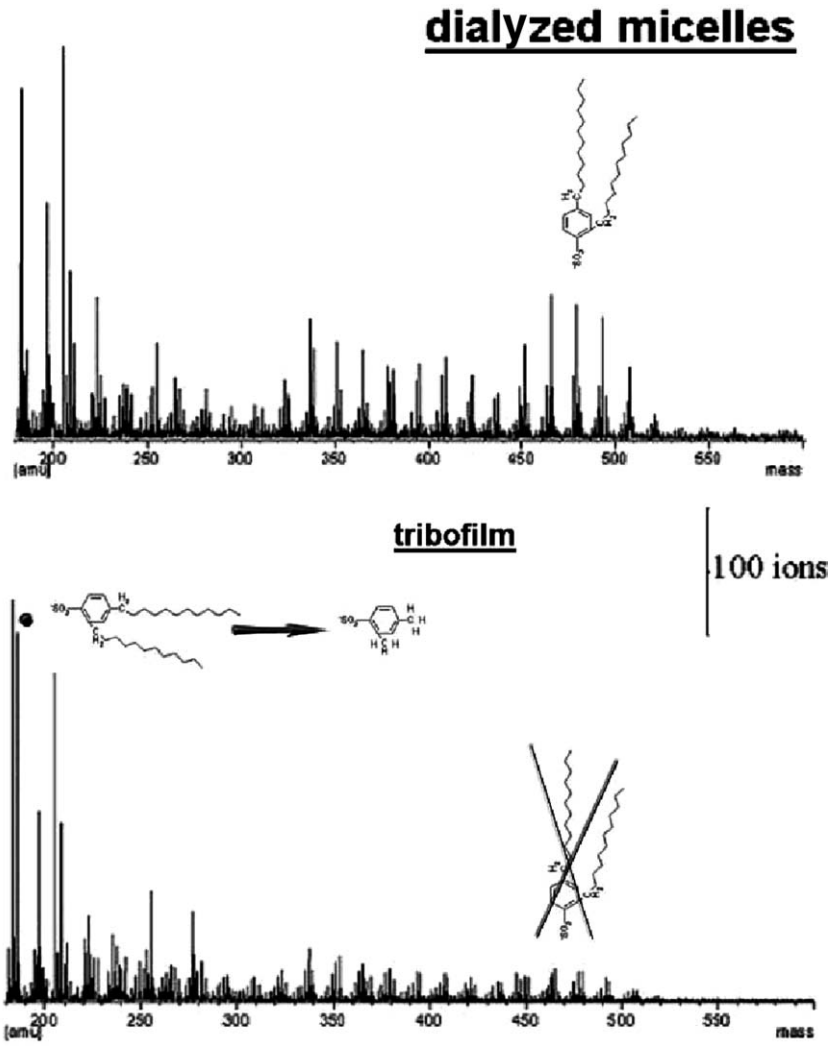

Figure 13. Negative ToF-SIMS spectra obtained as a comparison on dialyzed micelles and flat wear track after friction under UHV conditions.

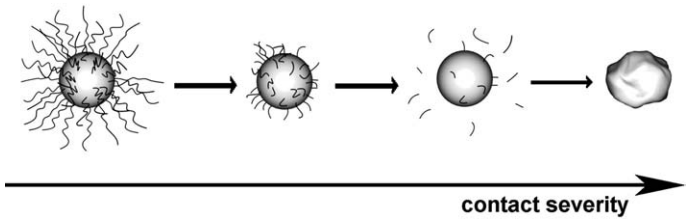

Figure 14. Proposed model for the evolution of dialyzed micelles in a tribological contact as a function of contact severity.

(3) Calcium carbonate grains crystallize in the calcite form and slide between each other due to the presence of carbon-rich joints.

4. Conclusion

By coupling several surface analyse methods, we have shown changes in micellar structure during friction due to high pressure and shearing. On one hand, surfactant chains are split and then expelled out of the tribofilm with increased contact severity. On the other hand, the amorphous calcium carbonate core crystallizes.

Thanks to several advantages compared to other anti-wear additives (e.g., ZDDP), overbased detergents seem to be very effective additives with no particular inconvenience except that, because of their detergent character, they clean rubbing surfaces and might prevent any other species from being adsorbed.

Acknowledgments

The authors would like also to thank the "Région Rhône-Alpes" (France) for financial support and Professor Kasrai (University of Western, Ontario) and Didier Parat (Science et Surfaces, Ecully) for helpful discussions on ToF-SIMS analyses.

References

[1] L. Cizaire, J.M. Martin and E. Gresser, Col. Surf. A (2003) (accepted for publication).
[2] J.M. Georges, Colloidal behaviour of film in boundary lubrication. Microscopic Aspects of Adhesion and Lubrication, Tribol. Series 7 (1991) 729.
[3] S. Giasson, Ph.D. dissertation; University of Paris VI, Paris, France, 1992.
[4] J.L. Mansot, M. Hallouis, J.M. Martin, Col. and Surf. A 75 (1993) 25.
[5] D. Mazuyer, A. Tonck, J.M. Georges, J.L. Loubet, Lub. Sci. 7 (1995) 309.
[6] F. Chinas-Castillo and H.A. Spikes, Trib. Trans. 43 (2000) 357.
[7] B. Delfort, M. Born, B. Daoudal, F. Dixmier and J. Lallement, Lub. Eng. 51 (1995) 981.
[8] P. Kapsa, J.M. Martin and J.M. Georges, Trans. ASME J. Lub. Technol. 102 (1981) 486.
[9] J.M. Georges, D. Mazuyer, J.L. Loubet and A. Tonck, Friction with colloidal lubrication in E.I.S.a, in *Fundamentals of Friction*, ed. H. Pollock (NATO Advanced Study Institute. Kluwer Academic Publishers, Brauwage, Germany, 1992).
[10] P. Hoornaert, D. Faure, M. Hallouis and J.M. Martin, *Proceeding of the Japan International Tribology Conference* (1990) p. 415.
[11] S. Giasson, D. Espinat and T. Palermo, Lub. Eng. 5 (1993) 91.
[12] T. Palermo, S. Giasson, T. Buffeteau, J.M. Turlet and B. Desbat, Lub. Sci. 8 (1996) 119.
[13] S. Giasson, T. Palermo, T. Buffeteau, B. Desbat and J.M. Turlet, Thin Solid Films 252 (1994) 111.
[14] M. Kasrai., W.N. Lennard, R.W. Brunner, G.M. Bancroft and J.A. Bardwell, Applied Surf. Sci. 99 (1996) 303.
[15] T. Le Mogne, J.M. Martin, C. Grossiord, *Proceedings of the 25th Leeds-Lyon*: *Lubrication at the Frontier*, D. Dowson, Elsevier (1999) p. 413.
[16] S. Barbon-Fernandez, C. Guerret-Piécourt, C. Grossiord, J.M. Martin, T. Le Mogne, B. Delfort and P. Gateau, ITC 2000 (2000).